

# The Effect of Interstitial Nitrogen Addition on the Structural Properties of Supercells of $\text{NdFe}_{12-x}\text{Ti}_x$

C. Skelland<sup>1</sup>, T. Ostler<sup>2</sup>, S. C. Westmoreland<sup>3</sup>, R. F. L. Evans<sup>1</sup>, R. W. Chantrell<sup>3</sup>, M. Yano<sup>4</sup>, T. Shoji<sup>4</sup>, A. Kato<sup>4</sup>, M. Winklhofer<sup>5</sup>, G. Zimanyi<sup>6</sup>, J. Fischbacher<sup>7</sup>, T. Schrefl<sup>7</sup>, and G. Hrkac<sup>1</sup>

<sup>1</sup>College of Engineering, Mathematics and Physical Sciences, University of Exeter, Exeter EX4 4QF, U.K.

<sup>2</sup>Faculty of Arts, Computing, Engineering and Sciences, Sheffield Hallam University, Sheffield S1 1WB, U.K.

<sup>3</sup>Department of Physics, University of York, York YO10 5DD, U.K.

<sup>4</sup>Toyota Motor Corporation, Toyota 471-8572, Japan

<sup>5</sup>Department of Biology and environmental sciences (IBU), Carl von Ossietzky Universität Oldenburg, 26129 Oldenburg, Germany

<sup>6</sup>Department of Physics, University of California at Davis, Davis, CA 95616 USA

<sup>7</sup>Center for Integrated Sensor Systems, Danube University Krems, E 2700 Wiener Neustadt, Austria

We investigated the effect of nitrogenation on  $3 \times 3 \times 2$  supercell structures of  $\text{NdFe}_{12-x}\text{Ti}_x$  from  $x = 0.028$  to  $x = 1.56$  ( $\sim 0.2\text{Ti}$  at. % to  $\sim 12\text{Ti}$  at. %). We used the molecular dynamics and Boltzmann probabilities to permeate titanium into  $\text{NdFe}_{12-x}\text{Ti}_x$  across the investigated range, before nitrogenating the minimum energy structures that resulted at each permutation step. By comparison of the nitrogenated and base structures, we found that the cohesive energy gains caused by nitrogenation are mainly due to a large asymmetry introduced into the  $c$  lattice parameter and the efficacy of nitrogenation decreases with increasing titanium at. %.

**Index Terms**—1:12 phase, cohesive energy, nitrogenation.

## I. INTRODUCTION

RESEARCH into permanent magnetic materials has been ongoing for over a century [1] and has seen rapid progress, moving from the high carbon steels of the mid-19th century to the rare earth magnets of the late 20th century. During this time, their increasing strength has allowed permanent magnets to be used in an increasing number of fields, particularly in electrical equipment such as MRIs and printers. However, it is their applicability in electrical engines and renewable energy technologies that are of most interest to us, as they are pivotal to the efficiency of these machines.

This series of technologies, using interior permanent magnetic motors in order to function, are instrumental in the world's effective transition to renewable energy. Therefore, it is important that the magnets in these machines are as powerful and effective as possible.

A permanent magnet's performance is categorized by two main measures: first, its maximum energy product ( $BH_{\text{max}}$ ), and second, for high-temperature applications, its Curie temperature.

Currently, the highest performance permanent magnetic material is  $\text{Nd}_2\text{Fe}_{14}\text{B}$ , which has  $BH_{\text{max}}$  of  $\sim 400 \text{ kJ/m}^3$  and a Curie temperature of 585 K as measured by Sagawa *et al.* [2]. However, although its performance is so far unsurpassed at low temperature, within the temperature range of electrical

engines, 435–455 K, its relatively low Curie temperature means its saturation magnetization and magnetic anisotropy is significantly reduced, and therefore, its performance is negatively affected. The current main method of combatting this low Curie temperature is to raise it by substituting some of the structures neodymium with dysprosium. The problems with this are twofold: first, an overall decrease in magnetization due to dysprosium coupling antiparallel to the iron atoms in the structure, and second, a substantial increase in the material cost driven by the price of dysprosium, which is linked to its general scarcity and supply issues [3]. Therefore, there is, despite the scientific challenges, a great deal of political and economic pressure to develop new permanent magnetic materials, which can compete with the incumbent  $\text{Nd}_2\text{Fe}_{14}\text{B}$ , while having less reliance on expensive heavy rare earth elements (such as dysprosium), a naturally higher Curie temperature, and similar  $BH_{\text{max}}$ .

The  $\text{RT}_{12}$  ( $R$  = rare earth and  $T$  = transition metal) phase, which forms in the tetragonal  $\text{ThMn}_{12}$  structure, shown in the bottom-right corner of Fig. 2, is one of these new materials.

The phase's main issue is the intrinsic instability of its binary structure, which is remedied by the addition of a ternary element, giving a structure of the form  $\text{RT}_{12-x}\text{M}_x$  ( $M$  = Si, Ti, V, Cr, Mo, or W). Investigation by De Mooij and Buschow [4] in 1988 found that the  $\text{RFe}_{12-x}\text{M}_x$  series of phases were the most promising due to their inclusion of iron, which possesses a high magnetic moment of  $3.63 \mu\text{B}$ . Continued investigation of this phase by Yang *et al.* [5], using titanium for the ternary  $M$  element, found that absorption of nitrogen significantly affected the magnetocrystalline anisotropy of the investigated structures, improving their magnetic properties. One of the investigated structures,  $\text{NdFe}_{11}\text{TiN}$ , was found to possess a

Manuscript received November 5, 2018; revised May 12, 2019; accepted May 23, 2019. Date of publication June 21, 2019; date of current version September 18, 2019. Corresponding author: C. Skelland (e-mail: cs502@exeter.ac.uk).

Color versions of one or more of the figures in this article are available online at <http://ieeexplore.ieee.org>.

Digital Object Identifier 10.1109/TMAG.2019.2920214

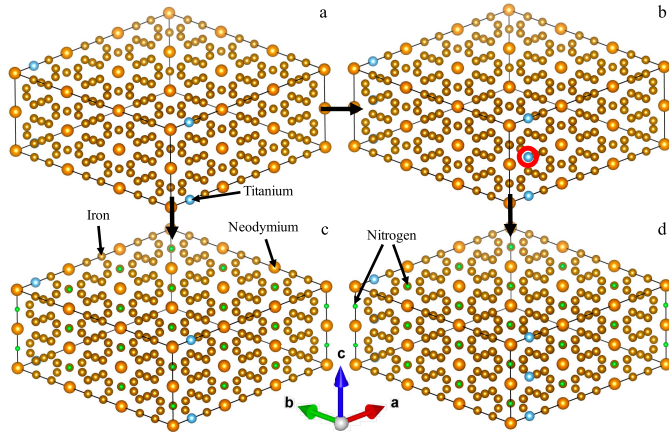


Fig. 1. Process by which atomic positions are filled with titanium, which can be seen following the arrow from (a) to (b). Then, the addition of interstitial nitrogen, shown in (c) and (d), which follows the filling of titanium. The constituent elements are labeled, and the series of arrows in the bottom middle represents the different lattice directions for all the structures. The new titanium atom added to the structure moving from (a) to (b) is circled in red in (b). Supercell structure of (a)  $\text{NdFe}_{12-x}\text{Ti}_x$  with 0.2 Ti at.%, (b)  $\text{NdFe}_{12-x}\text{Ti}_x$  with 0.4 Ti at.%, (c) 0.2 Ti at.%  $\text{NdFe}_{12-x}\text{Ti}_x$  with interstitial nitrogen added to it, and (d) 0.4 Ti at.%  $\text{NdFe}_{12-x}\text{Ti}_x$  with interstitial nitrogen added to it.

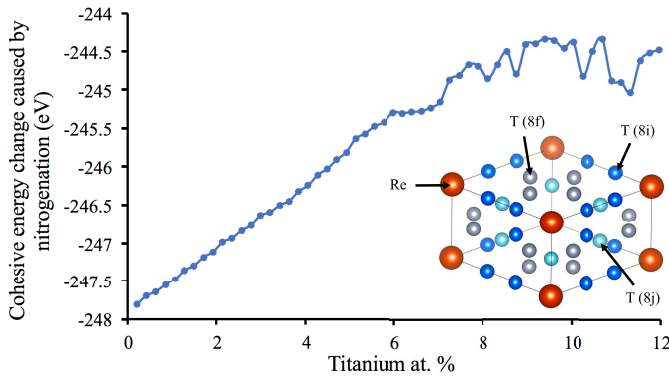


Fig. 2. Change in cohesive energy caused by the nitrogenation of a base  $\text{NdFe}_{12-x}\text{Ti}_x$  structure against titanium at. %. Bottom-right corner: diagram of a single unit cell of the  $\text{RT}_{12}$  structure, with the rare earth, and transition metal position labeled with Re, and T respectively. The Wyckoff positions of the transition metal are included in brackets.

Curie temperature of 740 K and estimated theoretical  $BH_{\text{max}}$  of  $\sim 430 \text{ kJ/m}^3$ , a vast improvement on the 585 K Curie temperature of  $\text{Nd}_2\text{Fe}_{14}\text{B}$  and only a slight downgrade from its theoretical  $BH_{\text{max}}$  of  $\sim 500 \text{ kJ/m}^3$  [6].

Computational investigation of the  $\text{NdFe}_{12}$ ,  $\text{NdFe}_{11}\text{Ti}$ , and  $\text{NdFe}_{11}\text{TiN}$  structures by Miyake *et al.* [7] has shown that nitrogenation of these structures affects their crystal electric field parameter  $A_{20}$ , the parameter that dictates the preferred direction of the rare earth elements' magnetic moments. Switching the base  $A_{20}$  of the  $\text{NdFe}_{12}$  structure from  $-83 \text{ K}$ , which gives in plane anisotropy, to  $413 \text{ K}$ , which gives uniaxial anisotropy in the  $c$  direction. This is repeated in the  $\text{NdFe}_{11}\text{Ti}$  structure whose base  $A_{20}$  of  $54 \text{ K}$  is enhanced by nitrogenation to  $439 \text{ K}$ . This switch to uniaxial anisotropy results in a higher magnetic anisotropy for the structure as a whole as the rare earth mediate their anisotropy to the transition metal elements. Further to this, nitrogenation increases the magnetic moment per formula unit of  $\text{NdFe}_{12}$  from  $24.89$  to

TABLE I  
LATTICE CONSTANT COMPARISON

Structure	Experimental			Calculated		
	a	b	c	a	b	c
$\text{NdFe}_{11}\text{Ti}$	8.574	8.574	4.907	8.554	8.553	4.853

Shows a comparison of the expected and calculated values for  $\text{NdFe}_{11}\text{Ti}$ , all values are given in Angstrom. The expected values for  $\text{NdFe}_{11}\text{Ti}$  can be found in [4]

$26.13 \mu\text{B}$ , and the magnetic moment of  $\text{NdFe}_{11}\text{Ti}$  from  $19.99$  to  $20.97 \mu\text{B}$ .

Our work is concerned with investigating the structural and cohesive energy changes caused by interstitial nitrogen addition, and the effect it has on the stability of the  $\text{NdFe}_{12-x}\text{Ti}_x$  structure. Using these results, we assess the possibility of a structural change causing the change in  $A_{20}$  seen by Miyake *et al.* [7].

## II. METHODOLOGY

Molecular dynamics simulations were used to calculate the structural properties of  $\text{NdFe}_{12-x}\text{Ti}_x$  structures. These simulations utilized the classical equations of motion and interatomic potentials to calculate the interaction between atoms in our investigated structures, and predict their final properties [8]. The property of greatest importance for the simulations is the cohesive energy, which is a measure of the amount of energy required to split a system from its crystalline form into its constituent parts. We use this property as a proxy for structural stability, with structures of lower cohesive energy being more stable. The modeling of atom-atom interaction by interatomic potentials is described in our previous work [9]. The interatomic potentials used in our simulations are either Morse potentials [10] or modified embedded atom models (MEAMs), which are derived from the results of *ab initio* simulations, and then verified by comparison with lattice constants from the literature. Our potentials' accuracy can be seen in Table I, which shows that our calculated lattice constants for  $\text{NdFe}_{12-x}\text{Ti}_x$  are within  $<1\%$  of the values found experimentally in the literature [5].

The Morse potentials used in this set of simulations are of the form

$$\Phi_{\text{sr}}(r_{ij}) = D_{ij}[(1 - e^{-\beta_{ij}(r-r_0)})^2 - 1] \quad (1)$$

where  $\Phi_{\text{sr}}(r_{ij})$  is the potential energy between atoms  $i$  and  $j$ ,  $D_{ij}$  is the disassociation energy of the bond,  $\beta_{ij}$  is a variable parameter determined from spectroscopic data,  $r$  is the distance between the atoms, and  $r_0$  is the equilibrium bond distance.

Our simulations proceed through a series of rounds, in which the minimum energy structure of given titanium at. % is found. Each round begins with a base atomic structure, taken either from a previous round or given to it at the start of the series. This base atomic structure has each of its available iron positions substituted with titanium in turn and the resultant structure simulated, and this process is shown graphically in the upper half of Fig. 1.

The simulations take the form of energy minimization calculations, which are performed using the Newton–Raphson method in General Utility Lattice Program [8] under constant pressure. The simulations proceed until a local energy minimum is reached, at which point the structures cohesive energy, lattice parameters, and atomic positions are output. The resulting series of simulated structures are then rank ordered by their cohesive energies, which are used along with Boltzmann probabilities to calculate the relative probability of each substitution position. The minimum energy structure, and therefore most probable position substitution, is chosen as the base structure for the next round of simulations. These rounds proceed until the desired stoichiometric percentage of titanium is achieved.

Once the desired stoichiometric percentage is reached, the base structures gained at the end of each round, which make up NdFe<sub>12-x</sub>Ti<sub>x</sub>'s minimum energy substitution path, have interstitial nitrogen added to their structures in the 2b Wyckoff positions, as shown in the bottom half of Fig. 1, before they are simulated again. By comparing the base and nitrogenated structures, the structural changes caused by nitrogenation can be investigated.

### III. RESULTS

Simulating the base  $3 \times 3 \times 2$  supercell structure of NdFe<sub>12</sub> gives base lattice parameter sizes of 25.5 Å for *a* and *b* and 9.7 Å for *c*, along with the cell angles of 90° in all cases. Our previous research [11] has shown that of the potential subsets of positions that titanium can substitute into, it has a clear preference for the 8i Wyckoff position subset, over the 8j, and 8f subsets, labeled on the crystal structure shown in the bottom right of Fig. 2. Therefore, in order to save computational time, our simulations only allowed the 8i iron atoms to be substituted by titanium, a graph demonstrating the comparative probability of the position sets can be found in [11].

Nitrogenation's effect on NdFe<sub>12-x</sub>Ti<sub>x</sub> structures was investigated from ~0.2Ti at. % to ~12Ti at. %, which translates to an *x* range from ~0.028 to ~1.56, and these results are reported in the following.

#### A. Cohesive Energy Changes

The changes in cohesive energy caused by nitrogenation remain relatively consistent across the investigated range, with an average change of -245.7 eV, from the un-nitrogenated to the nitrogenated structure, which works out as -13.7 eV per formula unit. Although the change is reasonably stable across the range investigated, there is a noticeable trend of decreasing gains in cohesive energy as titanium at. % increases up to ~7.7Ti at. %. The decrease is  $\sim 1.1 \times 10^{-1}$  eV per 0.2Ti at. %, which equates to a decrease of  $\sim 6.1 \times 10^{-3}$  eV per 0.2Ti at. % per formula unit. The consistency of this trend begins to cease past ~7.7Ti at. %, and while the cohesive energy gained by nitrogenation still decreases with increasing titanium at. % (at  $\sim 4.5 \times 10^{-2}$  eV per 0.2Ti at. %), it does so in a non-linear manner, as shown in Fig. 2. Therefore, at higher titanium percentages, we can see that there are optimal stoichiometries for maximizing the stability of the structure by nitrogenation, which are not purely based on minimizing titanium at. %.

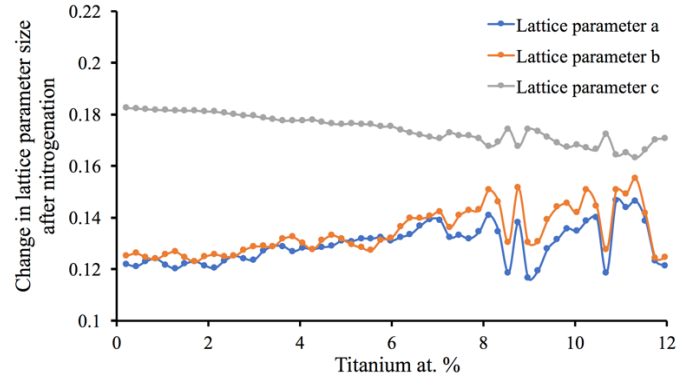


Fig. 3. Changes in lattice parameters *a*, *b*, and *c* caused by the nitrogenation of a base NdFe<sub>12-x</sub>Ti<sub>x</sub> structure against titanium at. %.

#### B. Structural Changes

Lattice parameter changes also show a consistent trend, with the difference between the maximum and the minimum size change caused by nitrogenation for *a*, *b*, and *c* lattice parameters being only 0.045, 0.044, and 0.026 Å, small compared to their average increases of 0.129, 0.134, and 0.174 Å, respectively. While the overall trend of expansion in *a* and *b* remains flat, there is a stable period from 0–7Ti at. % in which the expansion caused by nitrogenation increases by  $3.1 \times 10^{-4}$  Å per 0.2Ti at. %. After which point, the *a* and *b* lattice parameter changes become non-linear, as can be seen in Fig. 3. This is compared to the *c* lattice parameter change, which slowly decreases across the whole range by an average  $-2.15 \times 10^{-4}$  Å per titanium substitution. The trend of decreasing expansion in the *c* lattice parameter with nitrogenation as titanium at. % increases is likely the reason for the similar decreasing trend in cohesive energy gains.

As can be seen in Fig. 3, there is always a discrepancy between the size changes caused in lattice parameters *a* and *b*. This effect is further shown in Fig. 4(a), in which it can be seen that titanium substitution alone causes a similar discrepancy in the percentage change of *a* and *b* from their base values. This discrepancy is caused by the specific substitution position of the titanium element, whose substitution forces surrounding atoms out of equilibrium, causing the structure to expand to accommodate it, reach a new energy equilibrium. However, as titanium has broken the symmetry of the structure, it is energetically favorable that the lattice expansion occurs primarily in either the *a* or *b* lattice direction, dependent on the placement of the atom. The fluctuation in the percentage difference, caused by titanium substitution, in lattice parameters *a* and *b*, seen in Fig. 4(a), is due to the symmetric fashion in which titanium atoms fill the structure, filling an atom and then those similar to it in the *c* direction. This titanium fill pattern can be seen in Fig. 1, in which the second replacement titanium atom, in Fig. 1(b), fills a position similar to the first titanium filled in Fig. 1(a) in the *c* direction. This effect is magnified by the addition of interstitial nitrogen. It can be seen that the average percent change in lattice parameter *a*'s size is increased from ~0.022% to ~0.52%, after nitrogenation, while lattice parameter *b*'s average percent change is increased

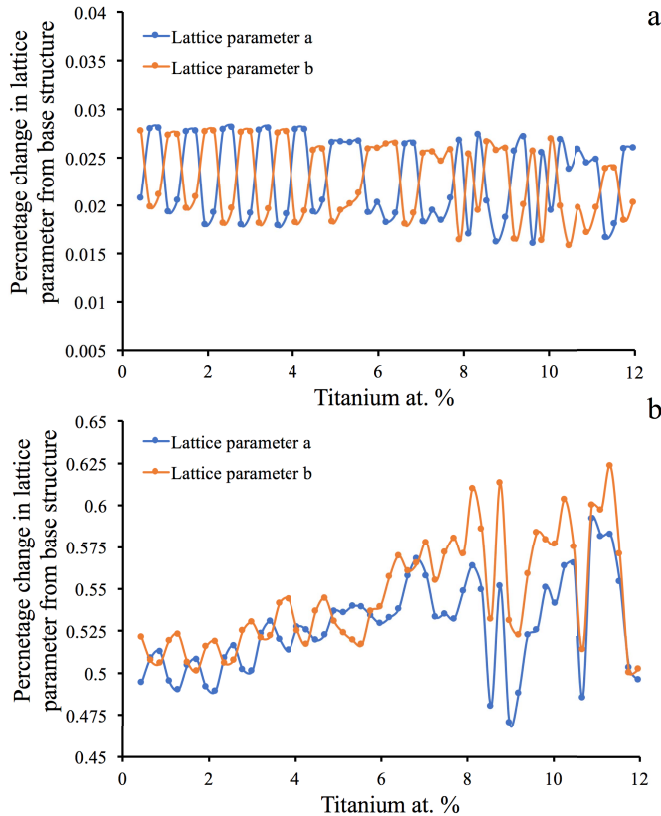


Fig. 4. (a) Percentage changes in lattice parameters  $a$  and  $b$  from the previous rounds selected base structure, caused by titanium substitution only. (b) Percentage changes in lattice parameters  $a$  and  $b$  from the previous rounds selected base structure, caused by titanium substitution and subsequent nitrogenation.

from  $\sim 0.022\%$  to  $\sim 0.54\%$ . In the un-nitrogenated structure, the difference between the percent change in lattice parameters  $a$  and  $b$  is on average  $7 \times 10^{-3}\%$ , and this is tripled by nitrogenation to  $0.022\%$ , inducing a larger asymmetry into the structure which is partially responsible for the large cohesive energy gains' nitrogenation causes.

As can be seen from Fig. 4(b), nitrogenation increases the  $b$  lattice parameter more on average than it does the  $a$  lattice parameter, and this is because, throughout this particular permutation on average, there are more atoms in positions which cause greater expansion in the  $b$  lattice parameter than those that cause it in the  $a$  lattice parameter. Therefore, due to the nitrogen atoms preferred positions, seen in Fig. 1, and its strong interaction with the titanium atoms, the addition of nitrogen causes a larger expansion in the lattice parameter that has more atoms expanding it, resulting in a similar but slightly shifted expansion pattern to that of titanium substitution alone.

This is generally correct up to  $\sim 7.7\text{Ti at.}\%$ , in which the titanium atoms follow a filling pattern that keeps them separated from one another in such a way that they do not exert a great amount of force on one another in the  $a$  and  $b$  lattice directions. However, beyond  $\sim 7.7\text{Ti at.}\%$ , the filling pattern changes, and further titanium substitutions prefer to lie much closer to the previous substitutions in the  $a$  and  $b$  lattice directions. By itself, this is not enough to cause

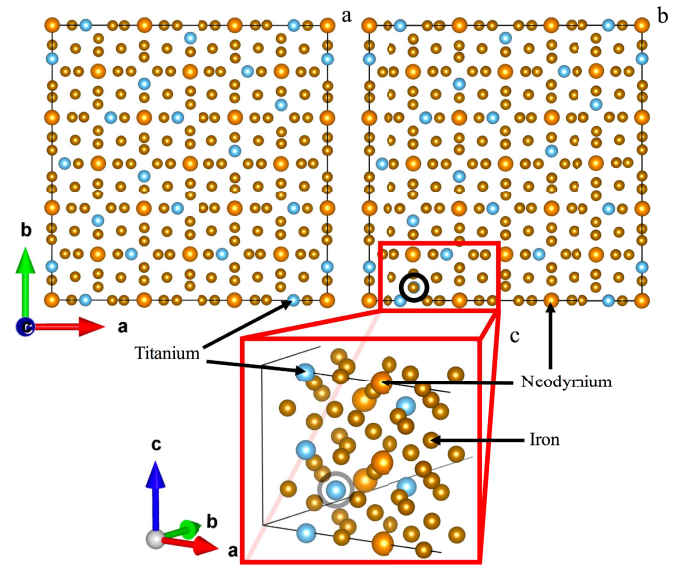


Fig. 5. (a) Planar view down the  $c$ -axis of the un-nitrogenated supercell atomic positions at the end of the first filling pattern,  $a$  and  $b$  axes indicated in the bottom-left corner of (a) and (b). (b) Planar view down the  $c$ -axis of the un-nitrogenated supercell's atomic positions of one titanium substitution into the second filling pattern—new titanium atom circled in black and hidden underneath an iron atom. (c) Side view of the volume local to the second filling atom, circled again, with the axis for this figure shown to the left of the diagram.

a significant change in the pattern seen in Fig. 4(a) during the first filling mode, in which the lattice parameter with the largest percentage size increase is purely dependent on the placement of the most recent titanium atom. The addition of interstitial nitrogen, however, forces the titanium atoms of the second filling pattern closer still to those of the first in the  $a$  and  $b$  directions, with this further reduced distance resulting in an equilibrium that has a more homogenous expansion in the  $a$  and  $b$  directions. Therefore, the expansion nitrogenation causes in  $a$  and  $b$  above  $7.7\text{Ti at.}\%$  are less dependent on the most recent titanium substitution and more dependent on how many atoms in total either lattice have expanding it. This can be seen in Fig. 4(b) in which the graph for the expansion of both lattice parameters  $a$  and  $b$  beyond  $\sim 7.7\text{Ti at.}\%$  follows the same pattern to a greater or lesser magnitude. The atomic positions of all the atoms within the first fill pattern, and then that of the first atom of the second fill pattern, are shown in Fig. 5(a) and (b) and (c), respectively, to illustrate this point.

Finally, lattice parameter  $c$ 's percentage change is increased from  $\sim 0.017\%$  to  $\sim 1.78\%$ , an average increase of a factor of 100. The induced asymmetry due to nitrogenation is the main cause of the large cohesive energy gains. The reason for this large expansion in the  $c$  lattice parameter is obvious when looking at Fig. 1(c) or (d), and seeing the preferred placement of the nitrogen atoms is directly between neighboring neodymium atoms. This causes a loss of equilibrium that forces the neodymium atoms apart and results in an expansion of the whole structures  $c$  lattice parameter.

#### IV. CONCLUSION

Nitrogenation of  $\text{NdFe}_{12-x}\text{Ti}_x$  greatly reduces the cohesive energy of the structure in all investigated cases,

although its efficacy decreases slightly as the titanium at. % increases. However, its non-linear behavior at higher titanium percentages, seen in Fig. 3, may be exploitable as a means of effectively stabilizing the structure by nitrogenation, with lower titanium at. % than one might expect from the assumption nitrogenation's effect that has a linear reliance on titanium at. %.

Investigation of the structural changes caused by nitrogenation indicates that the main method by which its cohesive energy gains are achieved is the large asymmetry induced in the *c* lattice parameter and a relative minor asymmetry induced in the *a* and *b* parameters. As the gain in cohesive energy nitrogenation causes is very large, we believe that it is sufficient to allow the infiltration of titanium and nitrogen into the system. However, it should be pointed out that lowering the titanium at. % is crucial due to the high formation energy involved in replacing iron with titanium in a 1:12 phase, compared to the 1:12 phase with nitrogen. Therefore, further in-depth investigation of the non-linear cohesive energy gains caused by the structures' second filling pattern should be undertaken, to see how they are related to the accompanying structural changes, in order to find a path to a method which stabilizes the structure at lower titanium at. %.

As the gain in cohesive energy with titanium and nitrogen is accompanied by a structural change, we infer the crystal electric field parameter changes due to the changing distance between the rare earth and iron atoms, resulting in a reorientation of the magnetic moments in the unit cells. This is supported by the fact that the titanium has an asymmetric site probability distribution [11]. Meaning its substitution for iron induces an asymmetry in the exchange between the rare earth-iron and iron-iron sub-lattices. This occurs due to the screening effect of the replacement titanium, which sits preferentially on sites directly next to the rare earth. Its position therefore weakening the nearest neighbor exchange and thereby enhancing the contribution of the next nearest neighbor spins, leading to a tilting of the rare earth magnetic moment with respect to the total magnetic moment in a pure 1:12 phase, changing the magnetocrystalline anisotropy. It is

by this method that the cohesive energy gains caused by the substitution of titanium, and subsequent nitrogenation, result in a change in the structures' magnetic properties.

#### ACKNOWLEDGMENT

This work was supported in part by EPSRC under Grant EP/P02047X/1 and in part by the Toyota Motor Corporation. This work is based on results obtained from the future pioneering program "Development of magnetic material technology for high-efficiency motors" commissioned by the New Energy and Industrial Technology Development Organization (NEDO).

#### REFERENCES

- [1] J. D. Livingston, "The history of permanent-magnet materials," *JOM*, vol. 42, no. 2, pp. 30–34, 1990.
- [2] M. Sagawa, S. Hirosawa, H. Yamamoto, S. Fujimura, and Y. Matsuura, "Nd-Fe-B permanent magnet materials," *Jpn. J. Appl. Phys.*, vol. 26, no. 6, pp. 785–800, 1987.
- [3] M. Humphries, *Rare Earth Elements: The Global Supply Chain*. Washington, DC, USA: Congressional Research Service, 2013.
- [4] D. B. De Mooij and K. H. J. Buschow, "Some novel ternary ThMn12-type compounds," *J. Less Common Met.*, vol. 136, no. 2, pp. 207–215, 1988.
- [5] Y.-C. Yang, X.-D. Zhang, L.-S. Kong, Q. Pan, and S.-L. Ge, "Magnetocrystalline anisotropies of RTiFe<sub>11</sub>N<sub>x</sub> compounds," *Appl. Phys. Lett.*, vol. 58, no. 18, pp. 2042–2044, 1991.
- [6] S. Hirosawa, Y. Matsuura, H. Yamamoto, S. Fujimura, M. Sagawa, and H. Yamauchi, "Magnetization and magnetic anisotropy of R<sub>2</sub>Fe<sub>14</sub>B measured on single crystals," *J. Appl. Phys.*, vol. 59, no. 3, pp. 873–879, 1986.
- [7] T. Miyake, K. Terakura, Y. Harashima, H. Kino, and S. Ishibashi, "First-principles study of magnetocrystalline anisotropy and magnetization in NdFe<sub>12</sub>, NdFe<sub>11</sub>Ti, and NdFe<sub>11</sub>TiN," *J. Phys. Soc. Jpn.*, vol. 83, no. 4, 2014, Art. no. 043702.
- [8] J. D. Gale, "GULP: A computer program for the symmetry-adapted simulation of solids," *J. Chem. Soc. Faraday Trans.*, vol. 93, no. 4, pp. 629–637, 1997.
- [9] S. C. Westmoreland *et al.*, "Multiscale model approaches to the design of advanced permanent magnets," *Scripta Mater.*, vol. 148, pp. 56–62, Apr. 2018.
- [10] P. M. Morse, "Diatomic molecules according to the wave mechanics. II. Vibrational levels," *Phys. Rev. J. Arch.*, vol. 34, no. 1, p. 57, 1929.
- [11] C. Skelland *et al.*, "Probability distribution of substituted titanium in RT<sub>12</sub> (R= Nd and Sm; T= Fe and Co) structures," *IEEE Trans. Magn.*, vol. 54, no. 11, Nov. 2018, Art. no. 2103405.